Detection Paddy Field using dual Polarization SAR Sentinel-1 Data

Detection Paddy Field using dual Polarization SAR Sentinel-1 Data

D Dirgahayu[1], **I M Parsa**[1] **and S Harini**[1]

[1] Remote Sensing Application Center, Jln. Kalisari No. 8 Pekayon, Pasar Rebo, Jakarta

dede_dirgahayu03@yahoo.com

Abstract. Paddy field conversion monitoring is necessary conducted to ensure successful the harvest of rice. The monitoring can be done by using satellite data, both optical and radar data, which can cover a large area. In tropical area, cloudy day usually occurred, so that problems can't be handle with optical data. Utilization of radar data that can penetrate the cloud condition can solve the problem, either as a complement of optical data or used alone to monitor the paddy field conversion. The research was conducted to investigate the capability of Sentinel 1 SAR multi temporal data to detect paddy field based on growth phenology of rice crop. This research explores SAR Sentinel-1A data (C-band, VV and VH polarization) for several growing seasons in 2017 (January-December) to detect paddy fields in Subang Regency, West Java.Stacking layer is carried out prior to classification, time series image and polarization composite image (VH/VV), stacking maximum, minimum, mean and range values, standard deviation and taking sample training and statistical analysis. Taking sample training takes into account the phenology of rice plants (phases of paddy crop) using references to appropriate Landsat imagery. Classification is done by the time series algorithm, while the accuracy is calculated with Kappa coefficients from the 1: 5000 paddy field map reference. The results found that SAR data in dual polarization (HV, VV), and Polarization Index (PI= 1-NDPI) can be used to detect paddy field. The best overall accuracy was obtained from the Min,Max, and Mean of PI 87%, Mean VH polarization 78%, Standard Deviation VH polarization 76%, and Range polarization VH 74%.

Keywords: , Sentinel-1A, statical analysis, time series algorithm, paddy rice mapping

1. Introduction

Rice is one of the main foods in several countries, especially in Indonesia. As the main foodstuff for the community, the effort to monitor the area of rice fields needs to be done to support national food security. The best technique for mapping rice fields in a wide area is by utilizing remote sensing technology.

Constraints in interpreting natural resources for the tropics are the high percentage of areas covered by clouds. Utilization of satellite data with an optical sensor will produce cloud cover information which causes no information (not classified) so that it affects the calculation of paddy field area. Therefore,

the utilization of radar sensor data is one of the answers for these problems because it has advantages not affected by clouds.

This study examines how the ability of multi-recording SAR data to map rice fields. SAR data visualization is very different from optical sensor data, so SAR data is more difficult to use both for visual and digital land cover interpretation. However, there have been many studies that identify paddy fields by utilizing time series data with results of considerable accuracy [1-2] found a significant relationship between backscatter VH values on the age of rice plants using sentinel 1 satellite data on small rice fields. Sentinel 1 Satellite Data is also used [3] for identification of paddy field area and estimation of plant growth phase.

2. Method

2.1. Research Area

The research area is in Subang Regency, West Java, especially in rice fields with an area of 97.67 Ha. Geographically, the region is located between 6.175 N latitude and 107.930 E longitude (Figure 1). The study area was dominated by paddy rice fields covering 63,051 Ha and non paddy rice fields (settlements, water bodies, other vegetation, and other built areas) of 34,623 Ha. Overall, Subang Regency has an area of 77.949 Ha of irrigated rice fields and 6,621 Ha of non-irrigated rice fields, or 9.03 percent of the area of paddy fields in West Java Province [4].

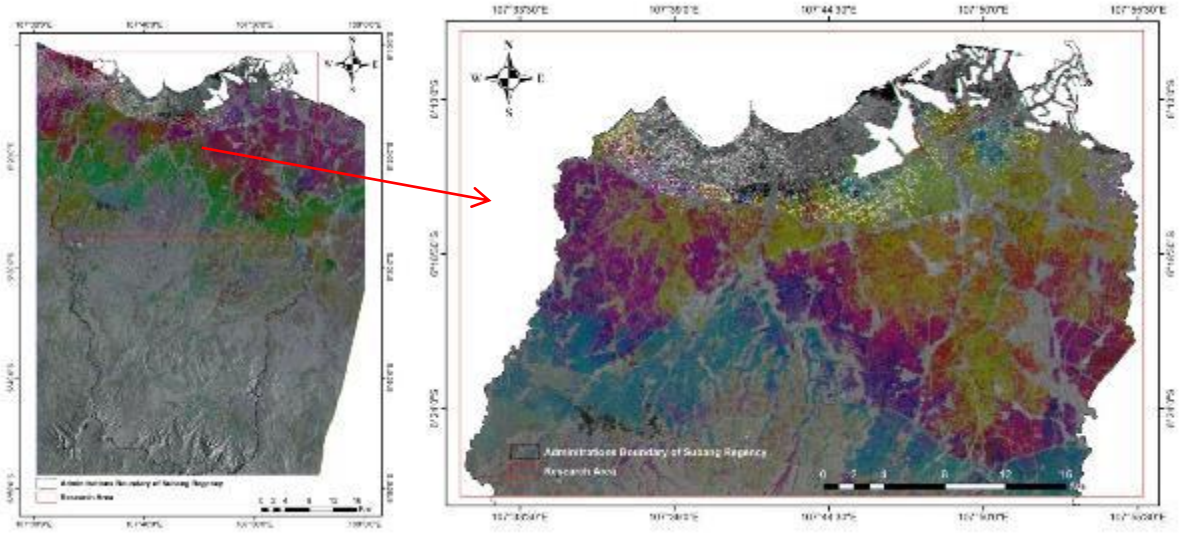

Figure 1. Research area

2.2. Data

The data used for the detection of paddy rice as can be seen in table 1.

Table 1. The data that used in this research

No	Tife of data	Date of data	Data usage	Source of data
1	Specification of Sentinel 1A data: 1. Resolusi 5 x 20 m, mode akuisis Interferometrik Wide (IW) 2. Data level 1 Ground Range	12 Daily, starting January 8, 2017 until December 22, 2017 (24 Data)	Decrease of time series algorithms for the detection of rice fields	European Space Agency (ESA).

No	Tife of data	Date of data	Data usage	Source of data
	Detection High (RGDH). 3. Dual Polarisasi VV, VH, dengan frekuensi 5.405 GHz. 4. Incidense Angel Range 30,56° – 45,91° 5. Descending Pase, orbit 149 6. Subset X = 4064, subset Y = 1957			
2	Paddy field map, scale 1:5000	Year 2017	Accuracy test	Geospatial Information Agency
3	Field survey	Year 2018	Validation	LAPAN
4	Google Earth	Year 2017	Validation	Google

2.3. Methodology

The time series algorithm used in this study is the development of algorithms that have been generated from previous researches [5-8]. In all three studies, the detection of paddy fields using backscattering values (σ^o) shows the difference for each class of land cover and land use. The backscattering value used is derived from VH and VV polarization and a combination of both. Determination of the value of back scattering is based on an understanding of the rice phenology, namely, planting time, generative phase, vegetative phase and harvest phase.

Determining the value of backscattering for the type of land cover and land use including paddy rice, is observing the dynamic changes of maximum and minimum backscattering values [7]. Meanwhile, for the detection of rice fields refers to the observation of the maximum and minimum backscattering values in accordance with the phenology of rice plants, starting from the planting day until the harvest day [6, 9]. In this study, the time series algorithm used is to use statistical analysis of the maximum and minimum backscattering values based on the phenology of rice plants, namely the maximum and minimum mean σ^o, the range of maximum and minimum σ^o, and the maximum and minimum standard deviations σ^o, at VH and VV polarization. The process of processing radar data and analyzing the detection of paddy rice can be seen in Figure 2.

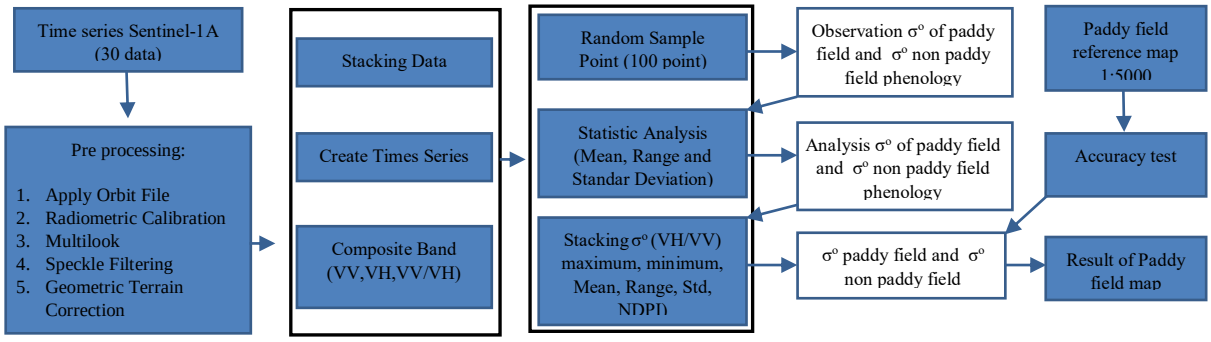

Figure 2. Research framework

Sentinel 1A SAR data is processed as much as 30 data. Pre processing of Sentinel-1A SAR data is to correct the SAR orbit so that it matches the orbit or the actual coordinates on the earth [10]. The correction also normalizes the recording angle. Radiometric correction is then performed to produce visual quality SAR data and pixel values that are in accordance with the real object σ^o reflection value [11]. The next step is to do geometric corrections. The correction actually has similarities with orbit

correction, but in geometric correction, SAR data has been adjusted to the topographic conditions and field coordinates using DEM (Digital Evaluation Model) data. In this study, DEM 1 sec with 30 meters resolution was used. Furthermore, image cropping (subset) is carried out according to the study area. The final processing step is speckle filtering with 3 x 3 lee filter method, namely the process of reducing the sharp random intensity of dark and bright areas in the SAR image [12]. The random intensity that occurs is a physical influence and not an atmospheric influence [10], so to increase the accuracy of observations and interpretations, a reduction in the effect is needed. The whole initial process, using the SNAP 6.0 open source application.

SAR images that have been generated through the initial processing process, then created (stack) for further time series dynamics of the σ^o value analysis for each land cover and land use class. Color gradations produced through band composites SAR images facilitate interpretation of land cover classes and land use. This study uses 100 sample points to observe changes in σ^o values starting from April until December 2017 (Figure 3). Through the dynamics of the σ^o value, then statistical processing is performed, including the mean value, standard deviation and range value to analyze the maximum value and minimum value of the closed class σ^o land and land use. Analysis of the maximum and minimum values of rice paddy fields depends on the accuracy of the observation and determination of the sample and the understanding of the phenology of paddy rice.

Some statistical values, namely the mean, range and standard deviation of rice paddy fields, are then processed in 18 SAR images, resulting in a map of paddy rice that has a specific σ^o value. The whole process uses the Arcmap 10.3 application. The assumptions used are in accordance with the previous research, which is using the phenology of rice paddy plants and the height size of rice plants according to the dynamics of the σ^o value. These assumptions are:

1. In the planting phase, the value of σ^o of paddy rice tends to be smaller than the generative and vegetative phase, can be written with the equation:
   σ^o planting phase < σ^o generative and vegetative phase

   In [13], explained that there are differences in the class height of paddy fields according to the planting phase to harvest (table 2).

2. In the generative phase, the σ^o value of paddy rice is greater than the planting σ^o phase but smaller than the vegetative phase, can be written with the equation:
   σ^o generative phase < σ^o vegetative phase,

3. In the vegetative phase, the σ^o value is greater than all the σ^o values in the phenology of the rice plant. In this phase, the value of σ^o is the maximum value, so that it can be written with the equation: σ^o vegetative phase > σ^o generative phase, σ^o vegetative phase > σ^o planting phase
4. In the harvest phase, the σ^o value is smaller than the vegetative phase but can have the same value of σ^o with the generative phase and can be written with the equation: σ^o harvest fase < σ^o vegetative phase, σ^o harvested phase ≥ σ^o generative phase

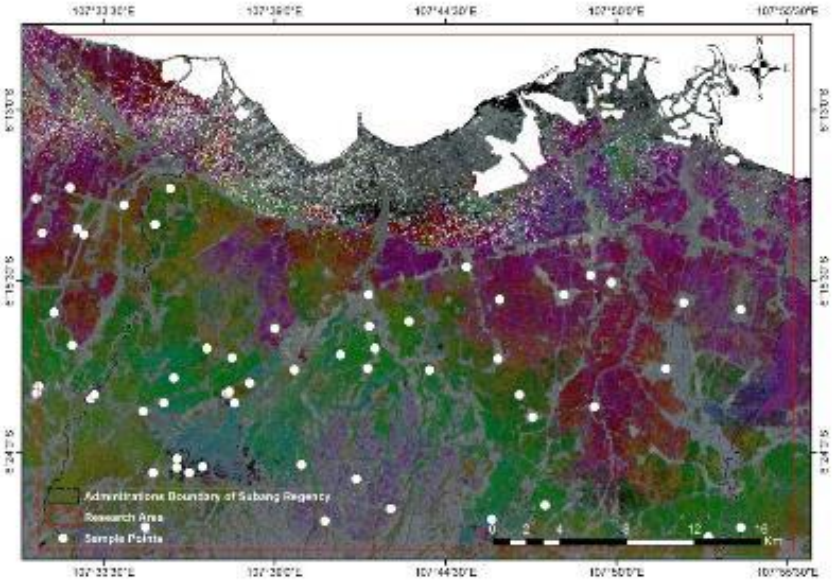

Figure 3. Random Sample Points

Determination of the assumptions above is also based on the height of the rice field plant according to the phenology of paddy rice (Figure 4) in the study of Ugsang, et al. (2017) [13], as in table 2 below.

Table 2. Description of the high size of paddy fields

No	High (Cm)	Paddy field phenology
1	< 21	Planting phase
2	21 – 60	Generative phase
3	60 – 78	Vegetative phase
4	> 78	Harvest phase

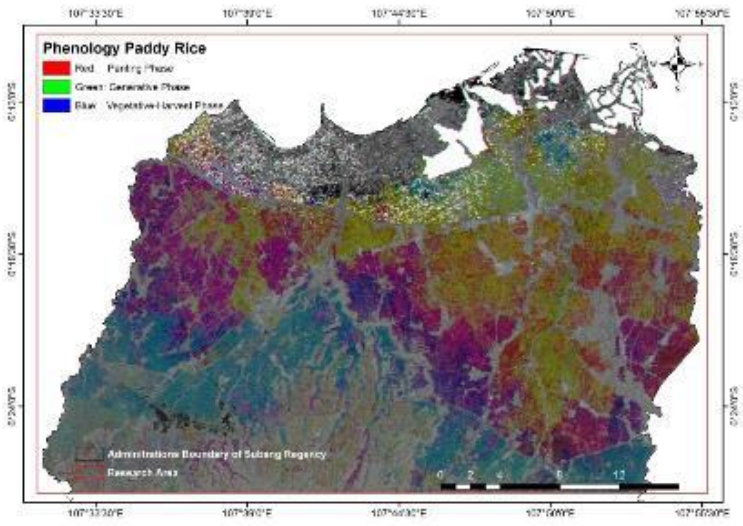

Figure 4. Phenology Paddy Rice Based on Composit SAR Data (60 Days)

In addition, according to [14], the growth of lowland rice plants is at the highest value the Vegetation Index is calculated 60 days after the planting date (generative and vegetative phases), and decreases until the harvest phase (rice growing period 105 - 120 days) The minimum σ° value can be used to use the planting date data, but in the planting phase, the σ° value has similarities to the σ° value of the water body class. However, in the harvest phase, the availability of paddy water begins to decrease, but the σ° value of paddy in the harvest phase is not used to calculate and detect paddy fields. To determine the minimum σ° value, an analysis of the harvest date is needed. Sentinel 1A has a daily 12 temporal resolution, it is very helpful to get the minimum σ° value of rice. The minimum σ° value of wet rice is determined 20 days after the planting date, or the minimum value of σ° is determined in the generative phase [6], so as to maximize the interpretation of paddy rice. At 20 days after the planting date, the paddy field canopy can be detected properly by radar. The last step is to test the accuracy, namely the determination of the Kappa coefficient value with the map reference using a 1: 5000 scale rice field map, sourced from the Geospatial Information Agency of the Republic of Indonesia.

3. Result and discussion

In the area of paddy rice research, there are planting dates and harvest dates that vary in each field. Variations in planting dates and harvest dates greatly influence the accuracy of the interpretation [6]. These problems can be reduced by taking an average value of Δ σ° for a minimum of 20 days after the planting date and a maximum value of Δσ° in the vegetative phase (60 days after the planting date), can be seen in figure 5 and figure 6. The minimum and maximum threshold values of Δ σ° in the land use and cover classes in this study can be seen in the following table.

Table 3. Maximum and minimum value of σ° for each class of SAR image classification results

No	Class	Polarization VH (dB)		Polarization VV (dB)	
		σ° Minimum	σ° Maximum	σ° Minimum	σ° Maximum
1	Urban	-19	-10	-12	-1
2	Bare land	-27	-8	-22	-2
3	Paddy field	-29	-11	-24	-3
4	Water body	-28	-19	-24	-11
5	Other vegetation	-21	-1	-14	-12

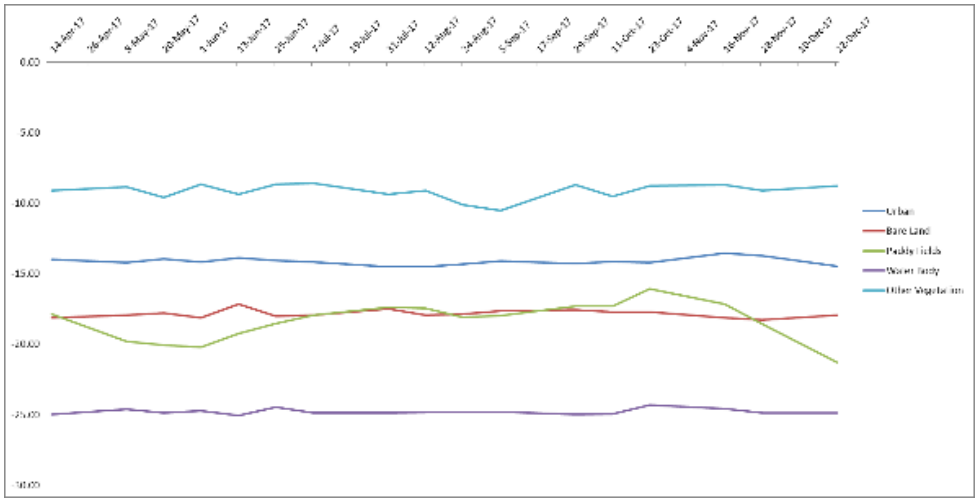

Figure 5. Graphic of Δσ° VH for each class, based on 100 sample points

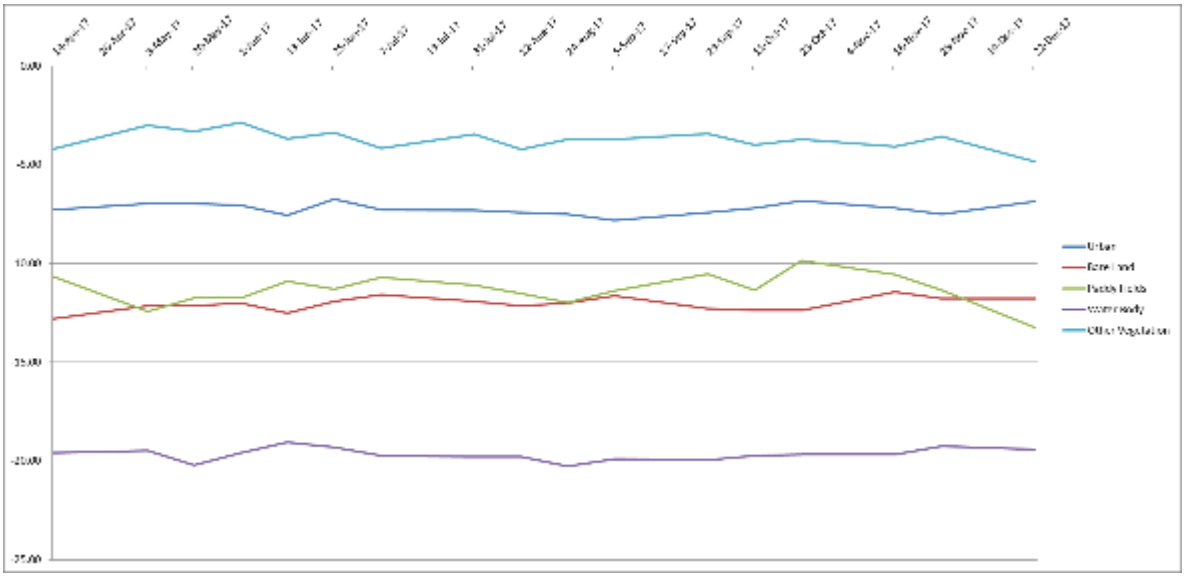

Figure 6. Graphic of $\Delta\sigma^o$ VV for each class, based on 100 sample points

Table 4. Minimum and Maximum value of $\Delta\sigma^o$ for each class of SAR image classification results

No	Class	Polarization VH (dB)		Polarization VV (dB)	
		$\Delta\sigma^o$ Minimum	$\Delta\sigma^o$ Maximum	$\Delta\sigma^o$ Minimum	$\Delta\sigma^o$ Maximum
1	Urban	-14.824	-12.824	-9.529	-3.250
2	Bare land	-11.471	-10.471	-7.176	-4.059
3	Paddy field	-20.176	-15.706	-13.882	-9.118
4	Water body	-26.235	-20.647	-21.941	-15.176
5	Other vegetation	-11.176	-2.471	-3.706	10.412

Table 5. Maximum and minimum standard deviation value of $\Delta\sigma^o$ for each class of SAR image classification results

No	Class	Polarization VH (dB)		Polarization VV (dB)	
		$\Delta\sigma^o$ Minimum	$\Delta\sigma^o$ Maximum	$\Delta\sigma^o$ Minimum	$\Delta\sigma^o$ Maximum
1	Urban	0.7717	1.7150	0.6063	1.7405
2	Bare land	0.7019	1.6627	0.8828	2.3856
3	Paddy field	1.6627	5.1990	1.1180	4.8462
4	Water body	0.7524	1.4552	0.8269	2.8556
5	Other vegetation	0.7998	1.9117	0.8944	2.3594

The distribution of σ^o values in each statistical analysis shows diversity. The maximum and minimum σ^o value of each class is the extraction of 100 sample points in SAR images. Determination of the mean value, standard deviation and maximum / minimum range based on the time series sample values from April to December 2017. The results of the field survey indicate that the planting date begins in the last week of April 2017. From the results, the maximum σ^o threshold value can be determined and minimum σ^o and adjusted to the phenology of paddy rice.

Table 6. Summary of minimum and maximum thresholds value of $\Delta\sigma^o$ for each class of paddy rice

No	Parameter	Minimum	Maximum	Algorithm
1	$\Delta\sigma^o$ Mean VH	-26.2974	-5.1822	($\Delta\sigma^o$ Mean VH ≤ -5.1822)

No	Parameter	Minimum	Maximum	Algorithm
2	$\Delta\sigma^o$ Mean VV	-22.1521	3.5816	& ($\Delta\sigma^o$ mean VH ≥ -26.2974 ($\Delta\sigma^o$ Mean VV ≤ 3.5816) & ($\Delta\sigma^o$ mean VV ≥ -22.1521)
3	$\Delta\sigma^o$ Range VH	2.3158	18.3039	($\Delta\sigma^o$ Range VH ≤ 18,3039) & ($\Delta\sigma^o$ Range VH ≥ 2.3158)
4	$\Delta\sigma^o$ Range VV	2.9499	23.0949	($\Delta\sigma^o$ Range VV ≤ 23.0949) & ($\Delta\sigma^o$ Range VV ≥ 2.9499)
5	$\Delta\sigma^o$ Standar Deviasi VH	0.7436	5.4177	($\Delta\sigma^o$ Stadev VH ≤ 5.4177) & ($\Delta\sigma^o$ Stadev VH ≥ 0.7436)
6	$\Delta\sigma^o$ Standar Deviasi VV	0.7186	8.0279	($\Delta\sigma^o$ Stadev VV ≤ 8.0279) & ($\Delta\sigma^o$ Stadev VV ≥ 0.7186)

Composite results are based on field data and SAR data shows the phenology phase of rice plants (figure 4). The research area shows that there is a variety of planting and harvesting phases of rice fields. The raster composite in Figure 3 has represented the estimated age of rice plants starting from the planting phase to the maximum phase of vegetation (60 days). From these data can be taken the minimum and maximum threshold values of rice plants, and reduce the noise σ^o value from the cover and other land use classes.

The predetermined algorithm results in a classification of paddy rice from all SAR data (18 data and 36 for VH and VV polarization image). Based on previous research, the use of SAR data polarization results in a variety of object interpretations. Especially for rice plants, the use of VH and VV SAR data polarization has been carried out. VH polarization and Gaussian screening already use to determine the area of lowland rice plants in Europe with the highest accuracy of 93 percent in Spain [6]. Choudhury & Chakrabhorty (2006) use HH polarization to calculate the area of wet rice plants in India, with an interpretation of 97 percent. This study uses statistical calculations of mean, range and standard deviation to calculate the area of paddy rice plants based on $\Delta\sigma^o$ maximum and $\Delta\sigma^o$ minimum thresholds. Detection results can be seen in the following figure.

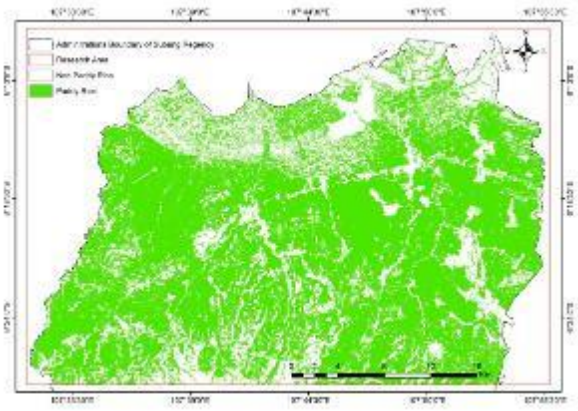

Figure 7. Classification results of paddy field using thresholds $\Delta\sigma^o$ maximum and minimum of Mean VH

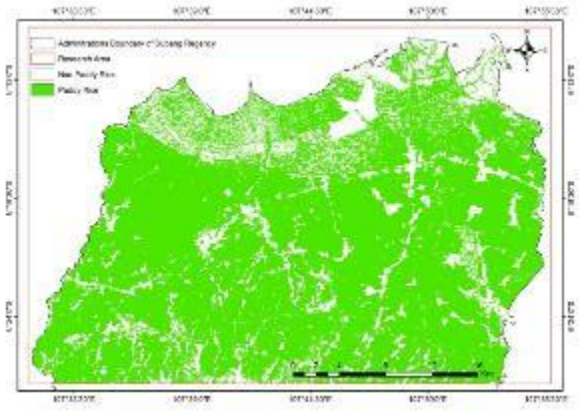

Figure 8. Classification results of paddy field using thresholds $\Delta\sigma^o$ maximum and minimum of Mean VV

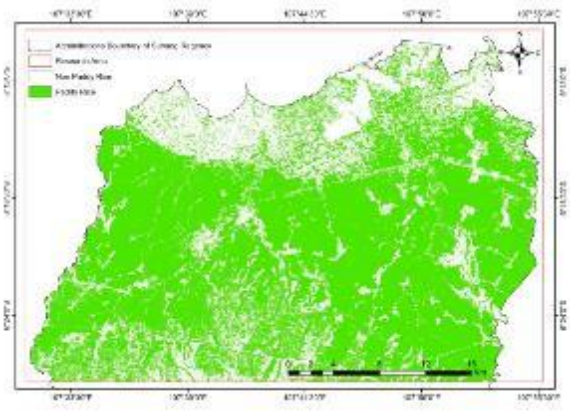

Figure 9. Classification results of paddy field using thresholds $\Delta\sigma^o$ maximum and minimum of Range VH

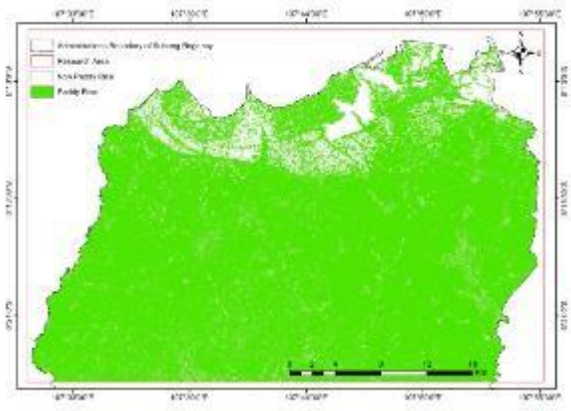

Figure 10. Classification results of paddy field using thresholds $\Delta\sigma^o$ maximum and minimum of Range VV

Figure 11. Classification results of paddy field using thresholds $\Delta\sigma^o$ maximum and minimum of Standard Deviation VH

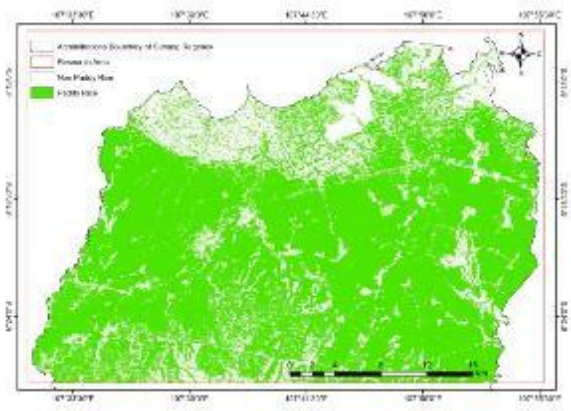

Figure 12. Classification results of paddy field using thresholds $\Delta\sigma^o$ maximum and minimum of Standard Deviation VV

Figure 7 - 12, shows the use time series of mean, range and standard deviation σ^o maximum and minimum algorithms. From those images, VH polarization tends to have a visual appearance similar to the 1: 5000 scale rice field maps.

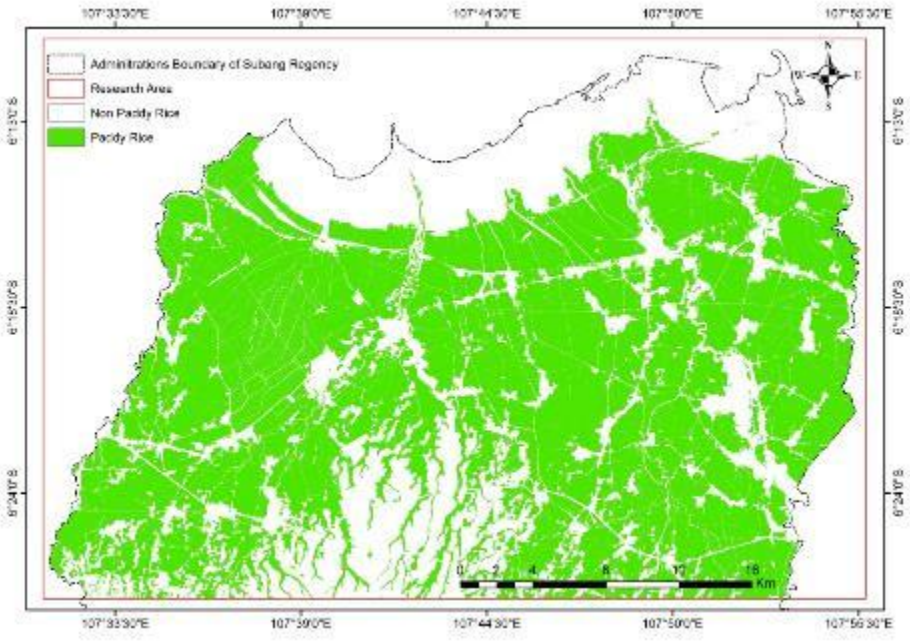

Figure 13. Map of 1: 5000 paddy field

Based on the accuracy test, it shows that the Kappa coefficient value varies for each algorithm used. The biggest Kappa coefficient is the mean VH algorithm and the smallest in the range VV algorithm. The overall results of using the time series algorithm can be seen in table 7.

Table 7. Kappa coefficient values

No	Statistical Parameter	Time Series Algorithms	Kappa coefficient (%)
1	$\Delta\sigma^o$ Mean VH	($\Delta\sigma^o$ Mean VH ≤ -5.1822) & ($\Delta\sigma^o$ mean VH ≥ -26.2974	78
2	$\Delta\sigma^o$ Mean VV	($\Delta\sigma^o$ Mean VV ≤ 3.5816) & ($\Delta\sigma^o$ mean VV ≥ -22.1521)	72
3	$\Delta\sigma^o$ Range VH	($\Delta\sigma^o$ Range VH ≤ 18,3039) & ($\Delta\sigma^o$ Range VH ≥ 2.3158)	74
4	$\Delta\sigma^o$ Range VV	($\Delta\sigma^o$ Range VV ≤ 23.0949) & ($\Delta\sigma^o$ Range VV ≥ 2.9499)	60
5	$\Delta\sigma^o$ Standard Deviation VH	($\Delta\sigma^o$ Stadev VH ≤ 5.4177) & ($\Delta\sigma^o$ Stadev VH ≥ 0.7436)	76
6	$\Delta\sigma^o$ Standard Deviation VV	($\Delta\sigma^o$ Stadev VV ≤ 8.0279) & ($\Delta\sigma^o$ Stadev VV ≥ 0.7186)	65
7	Min,Max, Mean PI = 1 - NDPI	PI_Min < 0.24 & PI_Max > 0.352 & PI_Mean >= 0.352 & PI_Mean <=0.392	87

Note : NDPI = (VV-VH)/ (VV+VH)

4. Conclusion

Detection of paddy field using SAR data has been widely carried out and has easy interpretation because it is not affected by cloud conditions. SAR image processing with various processing methods starting from the pre-process stage to the analysis greatly affects the accuracy of the interpretation results. In this study shows that the use of time series

algorithms sourced from statistical analysis of mean, range and standard deviation have varying degrees of accuracy. The use of VH polarization in all three statistical analyzes shows that the accuracy value is above 74 percent, whereas in VV polarization, the greatest accuracy value is only in the mean VV statistical analysis, while for standard deviation and range, the accuracy is below 70 percent. A better result to detect paddy field is using combination of VH and VV polarization, such as **Polarization Index (PI = 1-NDPI)** based on statistical multitemporal of NDPI [(VV-VH)/ (VV+VH)] during 1-3 years. The accuracy of observations on the phenology of rice plants also determines the accuracy of the classification results. In addition, the number of use of observation points in each class of land cover and use also has an important role. Accuracy and use of processing methods and the use of a combination of polarization VH, VV, HH, HV, need to be studied in order to get the best classification result.

Acknowledgments
We would like to thank all members of team for their cooperation in processing, analyzing results and other friends who have given their suggestions until the completion of this paper.

References
[1] Nuevo R U, Saludes R B, Dorado M A and Bantayan N C 2017 Monitoring of Rice in Small Paddy Fields Using Multi-Temporal, Sentinel-1 Data. https://www.researchgate.net/publication/321870352.
[2] Nuevo R U 2017 Monitoring of Rice in Small Paddy Fields Using Multi-Temporal Sentinel-1 Data. Conference Paper. October 2017 Conference: 38th Asian Conference on Remote Sensing.
[3] Torbick N, Chowdhury D, Salas W. And Qi J 2017 Monitoring rice agriculture across Myanmar using time series Sentinel-1 assisted by Landsat-8 and PALSAR-2. Remote Sens. 2017, 9, 119; doi:10.3390/rs9020119.
[4] Data Center and Development Analysis of West Java Province 2015 Wetland Areas and Types of Irrigation by Regency and City in 2015 in West Java. http://pusdalisbang.jabarprov.go.id/pusdalisbang/data-49-pertanian.
[5] Choudhury I and Chakraborty 2006 SAR Signature of Rice Using RADARSAT Data. International Journal of Remote Sensing. Vol. 27, No. 3, Februari 2006, 519-534; doi: 10.1080/01431160500239172.
[6] Nguyen D B and Wagner W 2017 European Rice Cropland Mapping with Sentinel 1 Data: The Mediterranian Region Case Study. Water. 2017, 9, 392; doi: 10.3390/w9060392.
[7] Chen C F, Son C R, Chang L Y and Chiang S H 2016 Rice Crop Mapping Using Sentinel 1A Phenological Metrics. Remote Sensing, Volume XLI-B8; doi: 10.5194/isprsarchives-XLI-B8-863-2016.
[8] Dong J and Xiao X 2016. Evolution of regional to global paddy rice mapping methods: A review. ISPRS Journal of Photogrammetry and Remote Sensing 119 (2016) 214-227.
[9] He Z, Li S, Wang Y, Dai L and Lin S 2018 Monitoring Rice Phenology Based on Backscattering Characteristics of Multi-Temporal RADARSAT-2 Datasets. Remote Sens. **2018**, 10, 340; doi:10.3390/rs10020340.
[10] ESA 2017 Sentinel 1 User Handbook.
[11] Danoedoro P 2012 Introduction of Digital Remote Sensing. Yogyakarta: Andi Offset.
[12] Sang H, Zhang J, Lin H, Zhai L 2014 Multi Polarization ASAR Backscattering From Herbaceous Wetland on Poyang Lake Region, China. Remote Sensing, 2014,6, 4621-4646; doi: 10.3390/rs6054621.

[13] Ugsang D M, Hinda H, Saito G 2017 C Band/HH Backscattering Characteristic of Paddy Fields: Implications for Rice Growth Monitoring. Remote Sens. 2017, 9, 119; doi:10.1173/rs9020119.
[14] Hernawati R, Harto A B and Sari D K 2017 Mapping of Paddy Patterns and Calendar Planting Using Remote Sensing Techniques. Reka Geomatika. ISSN 2338-350X No 2, vol. 2017.91.101.